

## Why Oceanic Dissipation Rates Are Not Lognormal

HIDEKATSU YAMAZAKI AND ROLF LUECK

*The Johns Hopkins University, Chesapeake Bay Institute, Baltimore, Maryland*

(Manuscript received 13 July 1989, in final form 7 June 1990)

### ABSTRACT

In their derivation of the lognormal probability density function for volume-averaged dissipation rates, Gurvich and Yaglom assumed explicitly that these dissipation rates are statistically homogeneous and that the averaging scale is small compared to the domain scale of the turbulent flow and large compared to the Kolmogorov scale. Estimates of dissipation rates in the oceanic thermocline reported by various researchers do not, in general, distribute lognormally because these datasets are often not homogeneous, nor is the averaging scale small compared to the scale of the turbulent patches. The conventional method of computing dissipation rates, a spectral technique, is incompatible with the assumptions for a lognormal distribution. Dissipation rates do distribute lognormally when they are computed with an alternative method that is consistent with the assumptions made by Gurvich and Yaglom. The shortest averaging scale that produced a lognormal distribution is three Kolmogorov length scales.

### 1. Introduction

The rate of dissipation of kinetic energy,  $\epsilon$ , is fundamental to our understanding of mixing in the ocean. The rate of dissipation is used to estimate a variety of parameters that characterize turbulent mixing including the vertical eddy diffusivity (Osborn 1980) and length scales such as the Kolmogorov scale,  $\eta \equiv (\nu^3 \epsilon^{-1})^{1/4}$ , and the Ozmidov scale,  $L_O \equiv (\epsilon N^{-3})^{1/2}$ , where  $\nu$  is the kinematic viscosity and  $N$  is the buoyancy frequency. Although values of  $N$  change moderately with depth in the thermocline, dissipation rates can change by several orders of magnitude over scales of a meter and, consequently, parameters that depend on  $\epsilon$  have a wide range of values. It is clear from past reports that dissipation rates have significant spatial and temporal variations, and choosing an appropriate value from a set of observations is rarely simple. For a finite set of observations spanning a region in space and time, should one choose the mean, or the mode, or a high-percentile value of  $\epsilon$ ? The statistical distribution of  $\epsilon$  should be a guiding factor. Dissipation rates are close to lognormal in surface and benthic mixing layers (Osborn and Lueck 1985a; Shay and Gregg 1986; Crawford and Dewey 1990) and above the core of the Pacific Equatorial Undercurrent (EUC) (Crawford 1982). However, dissipation rates deviate noticeably from a lognormal distribution in the thermocline (Lyubimtsev 1976; Osborn 1978; Osborn and Lueck

1985b; Lueck 1988; Yamazaki et al. 1990) and recent observations in the Pacific EUC are also not lognormal (Peters and Gregg 1988; Moum et al. 1989).

The discrepancy between the distribution of  $\epsilon$  in the thermocline and the lognormal distribution predicted by Gurvich and Yaglom (1967, hereafter GY) raises the question, "Is the lognormal theory of GY not applicable to a stratified fluid, or is the current methodology of computing  $\epsilon$  not consistent with the assumptions of GY?" We will argue for the latter case using two sets of data. We will show that conventional estimates of  $\epsilon$  in the thermocline form datasets that violate the important assumption of statistical homogeneity in the GY theory of lognormality (sections 2 and 3b), and that dissipation rates do follow a lognormal distribution when they are estimated with an alternative method that is consistent with the assumptions of GY (section 3c). Although our main concern is the lognormality of  $\epsilon$  in the thermocline the alternative method is applicable to other types of data. Further support for our alternative method is presented in the Appendix where we examine data from the Mediterranean outflow.

### 2. Lognormal theory: A review

The assumptions made by GY in their original derivation of the lognormal probability density function (pdf) for dissipation rates are crucial to understanding why estimates of  $\epsilon$ , particularly from the thermocline, frequently fail to follow a lognormal distribution. Because the details of the lognormal theory are rarely discussed in the context of oceanic observations, a brief summary is presented here.

*Corresponding author address:* Dr. Hidekatsu Yamazaki, Chesapeake Bay Institute, The Johns Hopkins University, The Rotunda, Suite 315, 711 W. 40th Street, Baltimore, MD 21211.

Yaglom (1966) applied the theory of breakage (Kolmogorov 1941a) to the energy cascade of turbulence, and GY introduced the scale-similarity law for  $\epsilon$ . A discussion of breakage and its relation to the log-normal pdf can be found in Crow and Shimizu (1988, ch. 3). The idea of breakage is the following. Let  $\epsilon(x)$  be a non-negative quantity defined only by local properties and let  $\epsilon_i$  be a volume average given by

$$\epsilon_i = Q_i^{-1} \int_{Q_i} \epsilon(x) dx \quad (1)$$

where  $Q_i \propto l_i^3$  is the averaging volume characterized by the length scale  $l_i$ . The quantity  $\epsilon_i$  is considered to successively break down into a smaller and similarly shaped volume  $Q_{i+1}$  contained within the volume  $Q_i$  and characterized by the length scale  $l_{i+1}$ . Successive values of  $\epsilon_i$  are related by the random breakage coefficient

$$\alpha_i = \epsilon_i / \epsilon_{i-1}, \quad i = 1, \dots, K \quad (2)$$

up to some stage  $K$  at which the values of  $\epsilon_i$  no longer fluctuate because of some physical limitation. The average value of  $\epsilon(x)$  in the entire domain  $Q_0 \propto L^3$  containing the breakage process is

$$\langle \epsilon \rangle = Q_0^{-1} \int_{Q_0} \epsilon(x) dx. \quad (3)$$

There are no restrictions on  $L$  other than that it must contain a breakage process, and  $L$  should not be confused with the scale of the energy containing eddies, to be discussed later. If there exists a range of length scales  $l_K < l_j < L$  in which the random variables  $\epsilon_j$  with different index  $j$  are *mutually independent* and *identically distributed* (IID) then the value of  $\epsilon_j$  in any particular volume  $Q_j$  is given by

$$\epsilon_j = \langle \epsilon \rangle \prod_{i=1}^j \alpha_i \quad (4)$$

and by

$$\log_e \epsilon_j = \log_e \langle \epsilon \rangle + \sum_{i=1}^j \log_e \alpha_i. \quad (5)$$

Finally, if  $\log_e \alpha_i$  satisfies the conditions of a stable distribution,  $\epsilon_j$  is lognormal by virtue of the central-limit theorem (Feller 1968). Gulovich and Yaglom implicitly assume that  $\log_e \alpha_i$  is a Gaussian. This assumption causes some physical inconsistency in higher order moments of turbulence statistics; but lower order moments, mean, and variance are predicted well by the GY model (Yamazaki 1990a). As it is with most statistical hypotheses, the critical condition is IID. The condition of mutual independence ultimately becomes invalid at some small scale because of the physical limitations to any breakup. "Identically distributed" means that the random variables  $\log_e \alpha_i$  must be drawn

from a *single* population and if, for some reason, the domain  $Q_0 \propto L^3$  contains breakages caused by more than one process,  $\log_e \alpha_i$  may not be identically distributed. This condition is frequently called statistical homogeneity, although its usage tends to be less rigorous than "identically distributed."

At an advanced state of the breakage process, that is, when  $j \gg 1$ , the length scales  $l_j$  form a nearly continuous set that is small compared to the domain scale  $L$ . Thus, one can associate any averaging scale  $r \ll L$  with a length scale  $l_j$  ( $j \gg 1$ ) and, using (5), express the volume average  $\epsilon_r$  by

$$\log_e \epsilon_r = \log_e \langle \epsilon \rangle + \sum_{i=1}^j \log_e \alpha_i. \quad (6)$$

Researchers making estimates of dissipation rates from microstructure profiles attempt to make  $r$  as small as possible, but computational considerations lead to values ranging from 0.5 m (Shay and Gregg 1986) to 4.0 m (Osborn 1978).

Gurvich and Yaglom's contribution is the application of the ideas of breakage to the theory of turbulence, and for convenience we will associate  $\epsilon_r$  with the volume-average rate of dissipation of kinetic energy. They were a little vague about the definition of the domain scale  $L$  and refer to it as "the typical scale of the mean motion." However, from their reliance on Kolmogorov's (1941b) notions of the inertial subrange, we take it that GY considered  $L$  to be the length scale of a single turbulent flow. In particular, GY considered  $\epsilon(x)$  to be isotropic and statistically steady in domains with scales small compared to  $L$ . They argued that at large Reynolds numbers there is a wide range of length scales satisfying the condition  $L \gg r \gg \eta_r = (\nu^3 / \epsilon_r)^{1/4}$  and that by "accepted hypothesis" the breakage coefficients in this range of length scales are mutually independent and identically distributed random variables. Their motivation for restricting the length scale,  $r$ , of the averaging volume was so that "the domain is small in comparison with a typical scale of inhomogeneities of the mean flow" and that "the domain is large as compared to the distances at which the molecular viscosity begins to be significant." Lastly, GY assumed that the probability of  $\epsilon_i = 0$  is zero, i.e., that the entire domain characterized by  $L$  contains dissipation. Yamazaki (1990a) discusses the detail of this statistic. Under these assumptions and restrictions, GY claimed that the volume-average rate of dissipation follows a lognormal distribution.

The problem with applying GY's theory of lognormality to thermocline observations is that the external length scale of patches of turbulence can be very small, particularly in the vertical direction. The thickness of the layers is frequently comparable to, and smaller than, the averaging scale  $r$  (0.5 to 4 m). For example, Gregg et al. (1986), Yamazaki and Lueck (1987), and Rosenblum and Marmorino (1990) have examined the

statistics of patch thickness and find that more than half of the turbulent layers are thinner than 2 m. If we interpret the domain scale  $L$  as the external length scale of a turbulent layer, in strict accordance with GY, then the condition  $r \ll L$  for statistical homogeneity is rarely satisfied in the thermocline. The de facto domain scale is the depth range of a set of observations, and if the individual estimates  $\epsilon_r$  in this set are identically distributed (represent a single population), their distribution should still be lognormal. However, the domain scale for a set of estimates is sometimes chosen arbitrarily (Baker and Gibson 1987) or with little concern for the external length scale of thermocline turbulence (Lueck 1988). Such datasets contain samples from unrelated turbulent layers mixed with specimens from regions that may not even be turbulent.

The importance of the domain scale was noted by Crawford (1982). His dissipation rates distributed lognormally when his dataset consisted exclusively of observations from above the core of the EUC (between 40 and 120 m). However, the distribution was not lognormal when the dataset was expanded to include estimates from the core and deeper water. Similar results were reported by Peters and Gregg (1988). The mean vertical shear is very small in the core and the physics of mixing in it must be quite different from the highly sheared flow above the core. The domain scale of a set of dissipation estimates is invariably large (of order 100 m) because 1) individual estimates are a spatial average over 0.5 to 4 m and 2) the set must contain a substantial number of estimates for statistical tests. Therefore, with only a few exceptions, such as the EUC, datasets from the thermocline are inconsistent with the assumptions and restrictions set forth by GY; that the domain scale is shorter than the external length scale of the turbulence and that the averaging scale is small compared to the domain scale. Such datasets are not homogeneous and we have no basis for expecting a lognormal distribution. The prerequisites on the averaging and domain volume for a lognormal distribution are extremely restrictive for data collected in the thermocline.

What is an appropriate choice for the domain scale,  $L$ , in the thermocline? It is any scale over which the volume-average dissipation rates are statistically homogeneous and, therefore, it is *not* the Ozmidov scale. The domain scale can be larger than the Ozmidov scale because homogeneity over a particular scale does not require overturning eddies at the same scale. The microstructure shear variance changes abruptly by several orders of magnitude at the upper and lower boundaries of a turbulent patch. Therefore, the thickness of a turbulent layer should be taken as the upper bound for the domain scale  $L$  until the internal structure of these layers is better understood. No clear guidance exists to determine  $L$  objectively. Gurvich and Yaglom assumed that the turbulence is isotropic over the averaging scale  $r$ . This is a convenient assumption

in a theoretical development, but it is not a prerequisite for a lognormal distribution. When the breakage coefficients are statistically independent and homogeneous, even if the turbulence is anisotropic, the measured dissipation rates should still be lognormal. Thus, conventional spectrally averaged dissipation estimates may sometimes appear lognormal; Gregg (1990, personal communication) found such a dataset.

In summary, by the theory of breakage and its application to turbulence, the volume average dissipation rate,  $\epsilon_r$ , has a lognormal pdf in a domain characterized by the length scale  $L$ , if the following three conditions are met:

- (i)  $\epsilon_r$  is statistically homogeneous in the domain,
- (ii) the averaging scale is *small* compared to the length scale  $L$ , and
- (iii) the averaging scale is *large* compared to the Kolmogorov scale,  $\eta$ .

### 3. Oceanic dissipation estimates

#### a. Data

To examine the question of lognormality in the thermocline, we will use data from one vertical profile (Fig. 1) and one quasi-horizontal profile collected over

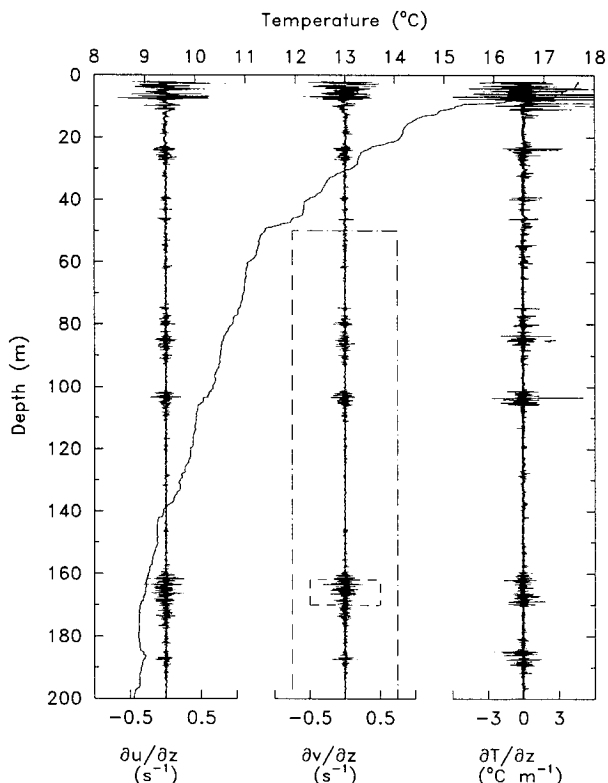


FIG. 1. Vertical profiles of  $\partial u/\partial z$  and  $\partial v/\partial z$ , temperature and its gradient. The  $\partial v/\partial z$  data between 50 and 200 m (large box) were used for the conventional dissipation estimates, while the segment between 162 and 170 m (small rectangle) was used in the alternative method.

the upper 200 m off San Diego, California. Details on the data collection and instrumentation are in Yamazaki and Lueck (1987) and Osborn and Lueck (1985b). While falling at an average rate of  $0.5 \text{ m s}^{-1}$ , the vertical profiler measured two orthogonal components of the vertical gradient of horizontal velocity,  $\partial u/\partial z$  and  $\partial v/\partial z$ , at a rate of 256 samples per second. The spatial sampling rate was  $512 \text{ m}^{-1}$ . The geographic orientation of the two velocity components is unknown and irrelevant, the nomenclature being used merely to distinguish the two signals. The sensors aboard the submarine *Dolphin* measured the horizontal gradients of vertical and athwartships velocity,  $\partial w/\partial x$  and  $\partial v/\partial x$ , at a rate of 512 samples per second while traveling at a speed of  $1.2 \text{ m s}^{-1}$ . The spatial sampling rate was  $427 \text{ m}^{-1}$ . The submarine was descending from a depth of 50 to 120 m with an average declination of  $6^\circ$ . The average buoyancy frequency between 50 and 120 m was  $N = 4.6 \text{ cph}$ . The detail of the hydrographic conditions for these datasets can be found in Yamazaki et al. (1990).

#### b. Conventional dissipation estimates

For our first test of lognormality, the dissipation rates were calculated in a conventional manner, namely, two-second blocks of data were Fourier transformed to produce variance spectra of shear and these spectra were integrated from 1 Hz to a frequency corresponding to one-half of the Kolmogorov wavenumber. The dissipation rate was calculated according to the isotropic turbulence formula:

$$\epsilon_r = 7.5\nu\langle s^2 \rangle \quad (7)$$

where  $\nu$  is the kinematic viscosity, which we take as  $1.3 \times 10^{-6} \text{ m}^2 \text{ s}^{-1}$  for the data discussed here,  $s$  is a component of the shear, and the angled braces indicate that the spectral integral is a spatial average. The averaging scale is two seconds, corresponding to a spatial scale of  $r \approx 1$  and  $2.4 \text{ m}$  for the vertical and horizontal profiles, respectively.

Ideally, one would like to integrate the spectrum from zero to infinity, but the sampling rate and noise considerations restrict us to a finite band of integration. The spectral method allows explicit control over the bandwidth used to estimate the shear variance and this is its main attraction. Noise in the measured shear signal above the upper limit of integration is excluded from the dissipation estimate (6), which increases its resolution. If the spectra follow the Nasmyth universal spectrum (Oakey 1982), then the spectral level is proportional to  $\epsilon^{3/4}$  and the upper limit of integration is proportional to  $\epsilon^{1/4}$ . In the thermocline  $\epsilon$  ranges approximately from  $10^{-10}$  to  $10^{-6} \text{ W kg}^{-1}$  and the spectral band of integration varies by an order of magnitude. An estimate of the amount of shear variance that is lost by using a finite upper limit can be obtained by assuming that the spectra follow, on average, the Nas-

myth universal shear spectrum. This is another attractive feature of the conventional method. Fifteen percent of the spectral variance is lost by ending the integration at one-half of the Kolmogorov wavenumber. The amount of signal variance lost due to the lower limit of integration depends on the rate of dissipation and is negligible for large rates. For the vertical profiles, 1 Hz corresponds to 2 cpm, while for the data collected with the submarine, 1 Hz corresponds to 0.8 cpm. For the very small rate of  $1 \times 10^{-10} \text{ W kg}^{-1}$ , the shear variance lost is 25% and 10% for the vertical and horizontal profiles, respectively, if the spectra follow the Nasmyth spectrum. At these levels of dissipation, velocity fluctuations are strongly influenced by stratification in the dissipation range of the spectrum and the vertical velocity spectra in low wavenumbers differ noticeably from the Nasmyth spectrum (Yamazaki 1990b). The dissipation rates reported here have not been corrected for the losses incurred by a finite bandwidth. Practical considerations, such as the length of data in the Fourier transform and low-frequency motions of the profiler, restrict the lower limit of integration to a finite value. Although details do vary, the spectral method described here is currently used by all microstructure researchers.

A vertical profile of the rate of dissipation estimated using  $\partial v/\partial z$  is shown in Fig. 2 (open circle). The minimum resolution of our method is  $5 \times 10^{-11} \text{ W kg}^{-1}$  and the estimates span more than 3 decades. As usual, the turbulence was "patchy" (see also Fig. 1) in the sense that there were layers thinner than 10 m with dissipation rates of order  $10^{-8} \text{ W kg}^{-1}$  separated by much thicker regions with rates of order  $10^{-10} \text{ W kg}^{-1}$ . Because the dissipative patches were well separated in space it is extremely unlikely that they resulted from a single process, and our dataset must contain samples from a number of different turbulent events. Even if we hypothesize that the turbulence was generated by a single *type* of process, the process could not have been started simultaneously in each layer, and the samples would come from different stages in the life cycle of this process and have differing statistical properties. Therefore, a typical profile of dissipation rates, such as shown in Fig. 2, is not homogeneous. For this dataset the domain scale is  $L = 150 \text{ m}$ . Our dataset meets two of the three conditions for lognormality. The averaging scale  $r = 1 \text{ m}$  is much less than the domain scale  $L = 150 \text{ m}$  (condition ii in section 2) and  $r$  is much larger than the Kolmogorov scale (condition iii), which is never more than 0.1 m in the ocean. However, our dataset does not meet the important condition of homogeneity.

A significant departure from lognormality is evident in a quantile-quantile plot (Fig. 3) where the logarithm of the empirical dissipation rates are plotted against the theoretical rates (hereafter a qq-plot; Chambers et al. 1983). This departure is similar to all previous reports. Although the departure from lognormality at

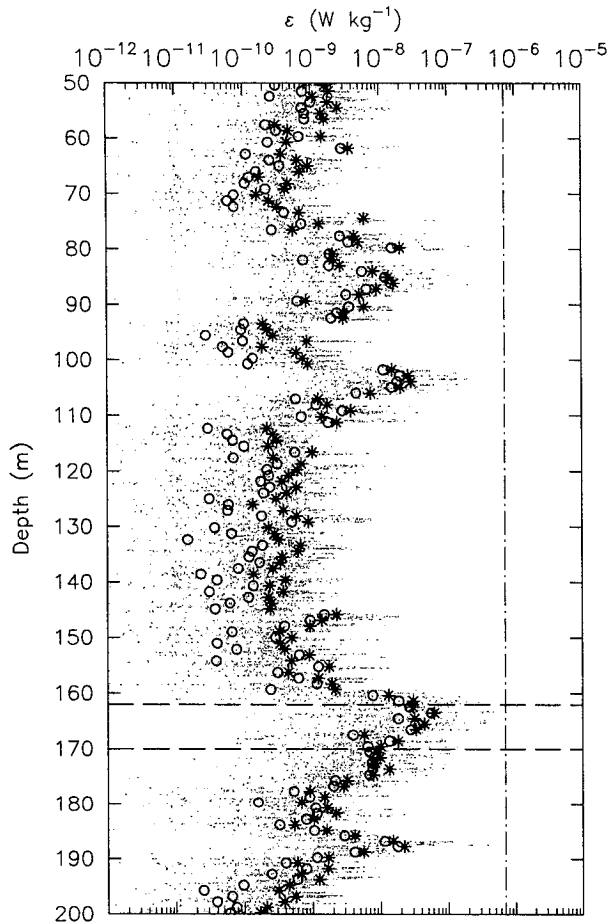


FIG. 2. Vertical profile of dissipation rates computed using  $\partial v / \partial z$ . The open circles are 1-m averages produced by the conventional method, the dots are the unsmoothed instantaneous rates and the asterisks are the instantaneous rates averaged over 1 m. The chain-dot line shows the dissipation rate corresponding to a Kolmogorov wavenumber of 120 cpm and the dashed lines delimit the 8-meter segment analyzed in section 3c.

rates smaller than  $10^{-10} \text{ W kg}^{-1}$  may be attributable to noise, the departure at large dissipation rates is not due to instrumental effects or other types of undersampling of the shear signal. The Kolmogorov–Smirnov test (hereafter, the KS test) rejected the null hypothesis that the dissipation estimates follow a lognormal distribution at a 5% significance level.

A quasi-horizontal profile taken with the submarine, and in close proximity to the vertical profile shown earlier, is displayed in Fig. 4 along with profiles of temperature,  $\sigma_t$ , and the depth of the boat. These data span a horizontal distance of approximately 630 m and a vertical distance of 70 m. The most dissipative event, near meter 240, was associated with intense fine-structure activity having a signature similar to an event interpreted by Itsweire and Osborn (1988) as a Kelvin–Helmholtz instability. The other regions of high dissipation had much smoother fine-structure in temper-

ature and density. Clearly a number of unconnected, and possibly different, mechanisms were responsible for the turbulence measured with the submarine, and the dataset shown in Fig. 4 is not homogeneous. Indeed a qq-plot of the dissipation rates (Fig. 5) departs significantly from a lognormal distribution and the KS-test rejected the dataset at a 5% level of significance.

### c. Instantaneous dissipation estimates

We will now attempt to extract a dataset that follows a lognormal distribution, and to do so, we will restrict our attention to a single turbulent layer in order to satisfy the assumptions in GY. We will use the shear signal  $\partial v / \partial z$  between 162 and 170 m, which is interior to a region of elevated turbulence spanning the depth range of 160 to 175 m (Figs. 1 and 2). This choice makes our domain scale  $L = 8$  m. The conventional spectral method provides only eight dissipation estimates. Although the data length used to compute the spectra can be shortened somewhat, this method cannot generate enough estimates for meaningful statistics. An alternative method is to use the square of every data point in the time series of  $\partial v / \partial z$  to compute the shear variance. This method produces a time series of  $(\partial v / \partial z)^2$  equal in length to the original shear signal. Spatial averaging is then accomplished by computing the means of a number of adjacent points, that is, through the decimation of the shear-squared time series into a shorter and smoothed series. This method provides explicit and generous control over the averaging scale at the price of very limited control over the spectral bandwidth. The bandwidth used to compute the shear variance can be controlled by filtering the shear data *before* squaring them, but the bandwidth cannot be varied among the individual estimates of the vari-

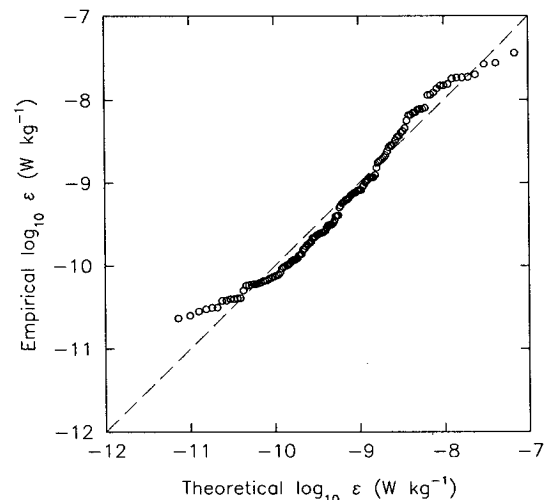


FIG. 3. The qq-plot of 1-m averaged dissipation rates computed with the conventional method using  $\partial v / \partial z$  data between 50 and 120 depth.

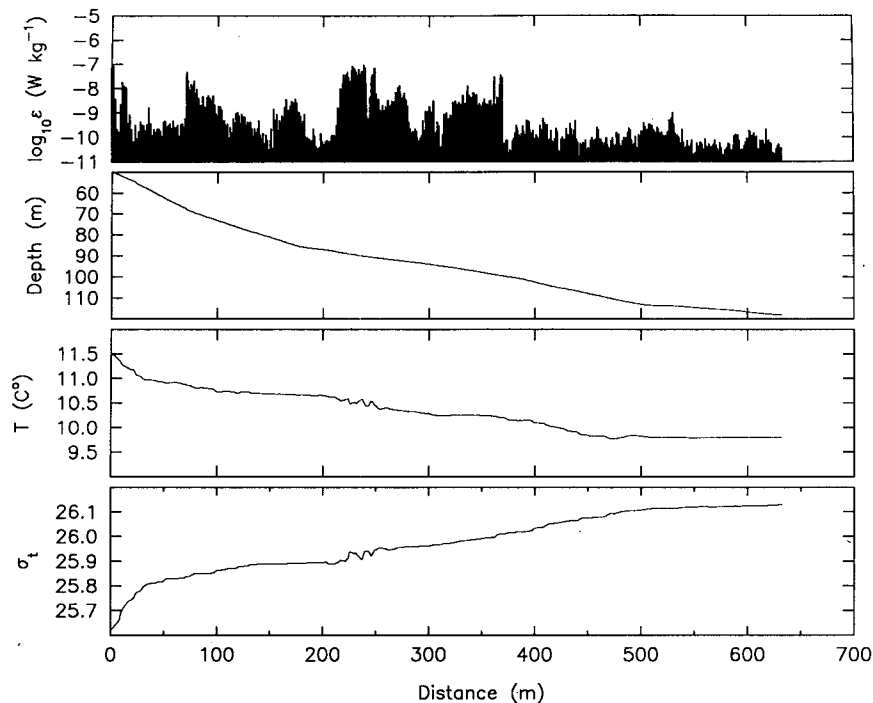


FIG. 4. Quasi-horizontal profile of dissipation rates averaged over 2.4 m and computed with the conventional method using  $\partial w/\partial x$ , along with profiles of depth, temperature, and sigma- $t$ .

ance. The maximum spatial resolution is determined by the sampling rate and is 0.002 m for the vertical profile. Although this “instantaneous dissipation” method may appear novel, it is the discrete equivalent of the analog, or continuous, methods used by the pioneers of turbulence research (Grant et al. 1962, Fig. 7). These and other researchers took the analog voltages

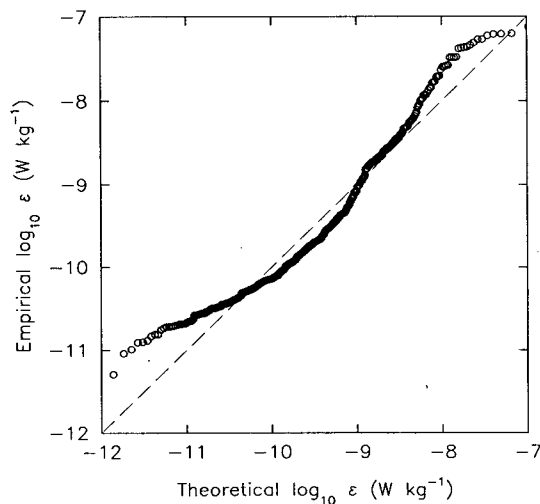


FIG. 5. The qq-plot of dissipation rate computed with the conventional method using  $\partial w/\partial x$  data collected from the submarine (Fig. 4). The averaging scale is 2.4 m.

produced by their velocity sensors, bandpass filtered the signals to reject drifts and high-frequency noise, squared this signal by various analog methods and, finally, averaged the variance using circuits with controllable time constants.

The spectrum of the 8-meter segment of  $\partial v/\partial z$  data between 162 and 170 m contains spurious peaks at wavenumbers above 120 cpm (Fig. 6). The two narrow peaks are associated with the power mains, while the broader peak between them has not been identified. The vertical profiler had a small amplitude wobble at a frequency of 0.3 Hz (Moum and Lueck 1985), although this is not particularly evident (in Fig. 6) because the shear signal was relatively large. We have low-pass filtered the shear data in the time domain with a nine-pole elliptic recursive filter (Antoniu 1979) set to reject signals above 120 cpm and high-pass filtered the data with a single-pole Butterworth filter set to attenuate signals below 0.2 cpm. The elliptic filter is extremely sharp and the effect of the two filters can be gauged by comparing the spectrum of the filtered and unfiltered signals (Fig. 6). The mean rate of dissipation for this 8-meter segment, using the conventional method, was  $2.4 \times 10^{-8} \text{ W kg}^{-1}$ . Based on this mean rate, the Kolmogorov length scale was  $\eta = 0.0031 \text{ m}$  and its wavenumber was 51 cpm. Because the high-wavenumber cut off of our filter is more than twice the average Kolmogorov wavenumber, our filter removes very little of the shear signal. The local dissipation rate

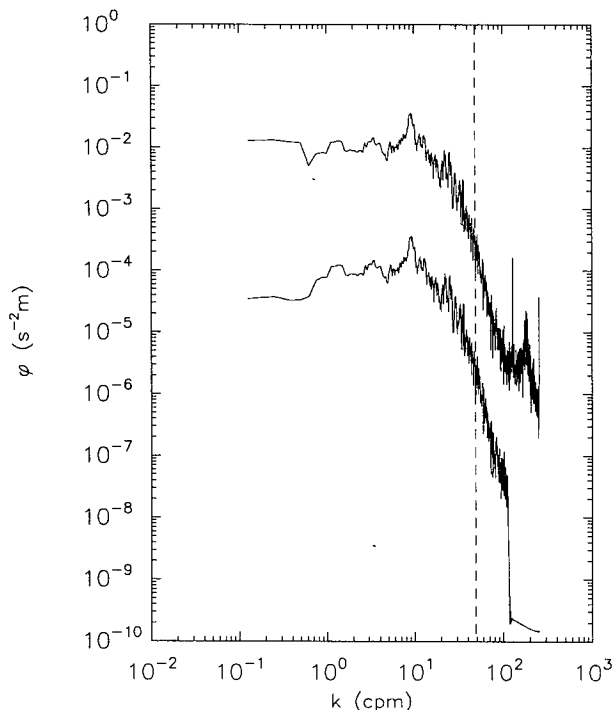


FIG. 6. Spectra of filtered and unfiltered  $\partial v/\partial z$  data between 162 and 170 m. The spectrum of the unfiltered data has been shifted up by two decades for clarity and the dashed line marks the Kolmogorov wavenumber.

within our 8-meter data segment was significantly larger than the mean rate, but as will be shown later, there was little loss of data even for local regions. The buoyancy frequency over the 8-meter segment was  $6 \times 10^{-3} \text{ s}^{-1}$ , and thus,  $\epsilon(\nu N^2)^{-1} = 510$ . By the criterion of Garrett et al. (1984), the turbulence was isotropic in the “dissipation” range of the wavenumber spectrum, a strong indication that the turbulence was homogeneous.

For comparison with the conventional method of computing dissipation rates, we have plotted (Fig. 2) a profile of the unaveraged instantaneous dissipation rates  $7.5\nu(\partial v/\partial z)^2$  showing every data point (512 per meter). Without smoothing, the instantaneous dissipation rates can be arbitrarily small and Fig. 2 shows only values larger than  $10^{-12} \text{ W kg}^{-1}$ . Very few dissipation rates exceed the rate corresponding to a Kolmogorov wavenumber of 120 cpm (Fig. 2, chain-dashed line)—our filter cutoff wavenumber. Decimating the instantaneous dissipation rates by averaging sequential groups of 512 estimates produced a subset of estimates averaged spatially over 1 m, a 512-point average, and these estimates should be comparable to the conventional ones. The two methods agree on the large dissipation estimates (Fig. 2, asterisks and circles), while for small dissipation rates, the spectral method produced estimates that are consistently smaller than the product of our alternative method. The difference

between the two methods at small dissipation rates reflects the advantage of the conventional method.

We have met two of the three conditions for lognormality—we have a dataset (between 162 and 170 m) that is very likely homogeneous (condition i in section 2) and the alternate method will allow us to keep the averaging scale small compared to the domain scale of  $L = 8 \text{ m}$  (condition ii). The final condition is the minimum averaging scale ( $r \gg \eta$ ), an issue intimately connected with the concept of statistical independence. By Kolmogorov’s third hypothesis (Kolmogorov 1962) the squared shears are mutually independent in the inertial subrange, but our sampling extended beyond this subrange and into the dissipation range of the shear spectrum. Therefore, the instantaneous dissipation estimates are not necessarily mutually independent. Our sampling scale of 0.002 m was smaller than the average Kolmogorov scale ( $\eta = 0.0031 \text{ m}$ ) and viscous smoothing should have rendered the estimates interdependent. Our instrumentation also performed some smoothing of the shear signal. The analog low-pass filter used for antialiasing purposes prior to digitization is not a factor because we used a very sharp 7-pole elliptic filter set to attenuate signals above the Nyquist frequency. However, the probes averaged the shear signal spatially and this process has been investigated at length by Ninnis (1984). To a very good approximation the probe acts as a “box-car” window with a width of 0.014 m and has its first null response at 175 cpm. Thus, for averaging scales comparable to and smaller than 0.014 m, the dissipation estimates were not statistically independent.

If we do not decimate our local dissipation rates, the estimates are not lognormal (Fig. 7a), undoubtedly because they do not satisfy condition (iii)—they are not mutually independent. To determine the amount of spatial averaging required to produce a lognormal set of dissipation estimates, we progressively decimated our instantaneous dataset (trying 2-point, 3-point, etc. averaging) and examined each decimated set for lognormality using the KS test. Decimation with 5-point averaging produced estimates that passed the KS test at a 5% level of significance (Fig. 7b). Thus, a spatial averaging scale of  $r = 0.010 \text{ m} \approx 3.1\eta$  produces a lognormal distribution for thermocline turbulence and quantifies the condition  $r \gg \eta$ , at least for this particular example. The averaging scale associated with 5-point averaging is comparable to the smoothing scale of the shear probe and, therefore,  $r = 3\eta$  is an upper estimate for the lower bound of  $r$  for lognormality. Had the spatial resolution of the shear probe been higher, a lognormal distribution may have been attained at a smaller averaging scale. All larger averaging scales up to and including decimation by 64-point averaging ( $r = 0.13 \text{ m} \approx 50\eta$ ) produced estimates that passed the KS-test (Fig. 7c). Averaging scales larger than 64 points were not attempted because at such scales the number of estimates is too small for a meaningful test.

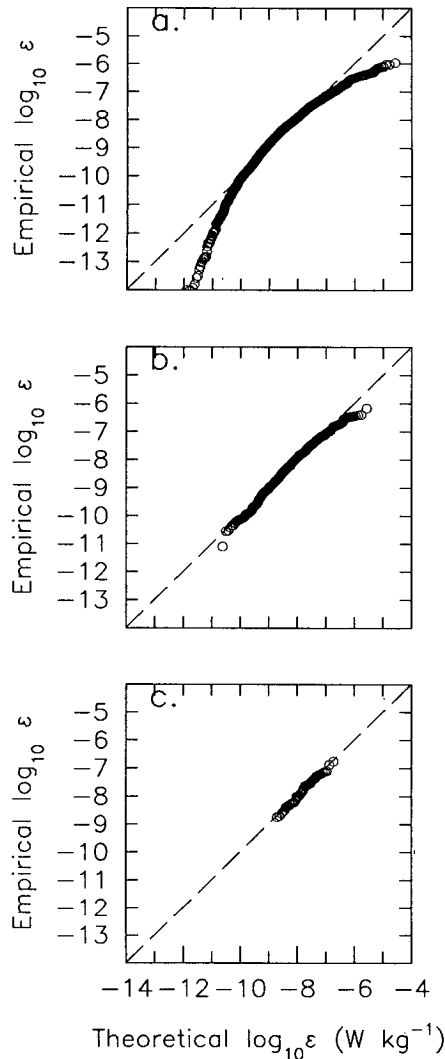


FIG. 7. The qq-plot of the instantaneous dissipation rate  $7.5\nu(\partial w/\partial z)^2$ ; (a) no averaging, (b) 5-point ( $r = 3\eta$ ) averaging, and (c) 64-point ( $r = 40\eta$ ) averaging.

The largest instantaneous dissipation estimate observed in our 8-meter segment was  $1 \times 10^{-6} \text{ W kg}^{-1}$  (Fig. 7a), and the Kolmogorov wavenumber corresponding to this rate is 130 cpm, which is larger than the cut-off wavenumber of our filter. If we can assume that the Nasmyth spectrum describes this dataset, then the loss of signal variance incurred by our filter is less than 3% for the largest estimate and even less for the smaller estimates. The signal variance lost due to spatial averaging by the shear probe is 21% using tables in Appendix C of Ninnis (1984). These tables quantify the total variance lost if the shear spectrum follows Nasmyth's universal spectrum and, hence, they overestimate the attenuation of instantaneous dissipation rates. Thus, the statistical distribution of the instantaneous and decimated dissipation rates are not sig-

nificantly affected by either probe smoothing or by the filtering of our data.

We also computed the instantaneous dissipation rates  $\epsilon = 7.5\nu(\partial w/\partial x)^2$  using the measurements taken with the submarine. We used a segment of data 16 seconds ( $L = 19 \text{ m}$ ) long (Fig. 8) that was imbedded in a larger turbulent region located near meter 240 of the entire horizontal profile shown in Fig. 4. This mixing layer was 5 m thick. The shear data were processed with the same method used for the vertical profile except that the filtering was different; no high-pass filter was used and the low-pass filter was set to 80 cpm. The spectrum of the selected 19-meter segment shows considerable signal contamination above 100 cpm (Fig. 9), which stems mostly from machinery aboard the boat (Osborn and Lueck 1985b). Rolling motions of the boat, which were small, had no effect on the  $\partial w/\partial x$  signal. The layer had an average dissipation rate of  $2.1 \times 10^{-8} \text{ W kg}^{-1}$ , a Kolmogorov length scale of  $\eta = 0.0032 \text{ m}$ , and a Kolmogorov wavenumber of 50 cpm (dashed line in Fig. 9). The buoyancy frequency in this layer was  $9 \times 10^{-3} \text{ s}^{-1}$ , hence,  $(\nu N^2)^{-1} = 200$ . By the criterion of Gargett et al. (1984), the turbulence was marginally isotropic in the dissipation range of the wavenumber spectrum. As before, the instantaneous dissipation rates are not lognormal when the dataset was not decimated (Fig. 10a). The least amount of spatial averaging that produced a dataset that passed the KS-test at a 5% level of significance was 4-point averaging, for which  $r = 0.0094 \text{ m} = 2.9\eta$  (Fig. 10b). All larger averaging scales up to and including 64-point averaging ( $0.15 \text{ m} = 47\eta$ ) passed the KS test at the same level of significance (Fig. 10c).

The margin between the average Kolmogorov wavenumber and the cutoff wavenumber of our filter was not as large for the horizontal profile as it was for the vertical profile and some loss of variance was incurred by our filtering. The largest instantaneous dissipation rate was  $3 \times 10^{-6} \text{ W kg}^{-1}$  (Fig. 10a) and the low-pass filter may have attenuated this value by approximately 17% and spatial averaging by the shear probe may have reduced this value by 30%. As was the

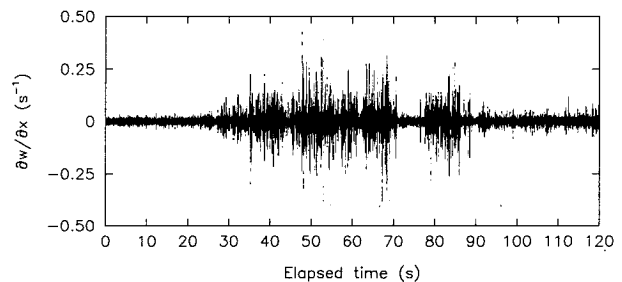


FIG. 8. Microstructure shear from a region near meter 240 in Fig. 4. The 19-meter long segment in the dotted rectangle was used to examine the statistics of the instantaneous dissipation rates  $7.5\nu(\partial w/\partial x)^2$ .



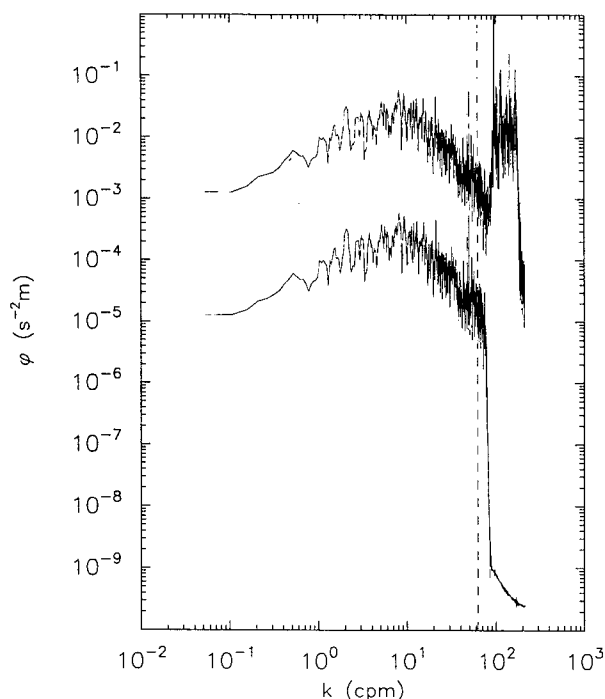


FIG. 9. Spectra of filtered and unfiltered  $\partial w/\partial x$  data from the 19-meter long segment identified in Fig. 8. The unfiltered data have been shifted up by 2 decades. The dashed line marks the Kolmogorov wavenumber.

case for the vertical profile, the statistical distribution of the dissipation rates from the 19-meter segment of the horizontal profile was not significantly affected by the probe smoothing or by filtering.

An averaging scale of  $3\eta$  was sufficiently large to produce a lognormal pdf using data from both the vertical and the horizontal profiler. This lower limit of  $3\eta$  is an order of magnitude smaller than the limit of  $36\eta$  suggested by van Atta and Yeh (1975) based on statistical independence. The fact that an averaging scale of 3 Kolmogorov lengths produced a lognormal distribution does not necessarily mean the estimates are statistically independent at this scale because the lognormal distribution may allow some degree of interdependence. Moreover, spatial averaging by the shear probe virtually guarantees statistical dependence at this scale.

#### 4. Discussion

The rate of dissipation of kinetic energy in the thermocline appears to be randomly distributed in space and time and is characterized by limited spatial and temporal scales. Dissipation rates estimated with conventional methods range over at least 3 decades, and  $\epsilon$  garnered from thermocline profiles is a highly skewed random variable. The lognormal distribution describes one particular family of skewed variables. Unfortun-

nately, conventional oceanic dissipation estimates generally violate the assumption of homogeneity in the GY theory of lognormality and this is the reason why (almost) all datasets fail statistical tests for lognormality. The restrictions for a lognormal distribution, as summarized at the end of section 2, are simply incompatible with conventional estimates of dissipation rates in the oceanic thermocline. The important role of homogeneity has been noticed in data collected in the EUC (Crawford 1982; Peters and Gregg 1988) and can also be seen by comparing mixing layer data against thermocline observations. Dissipation estimates drawn from surface mixing layers are close to lognormal, although they do not always pass statistical tests. Shay and Gregg (1986) measured dissipation rates in a con-

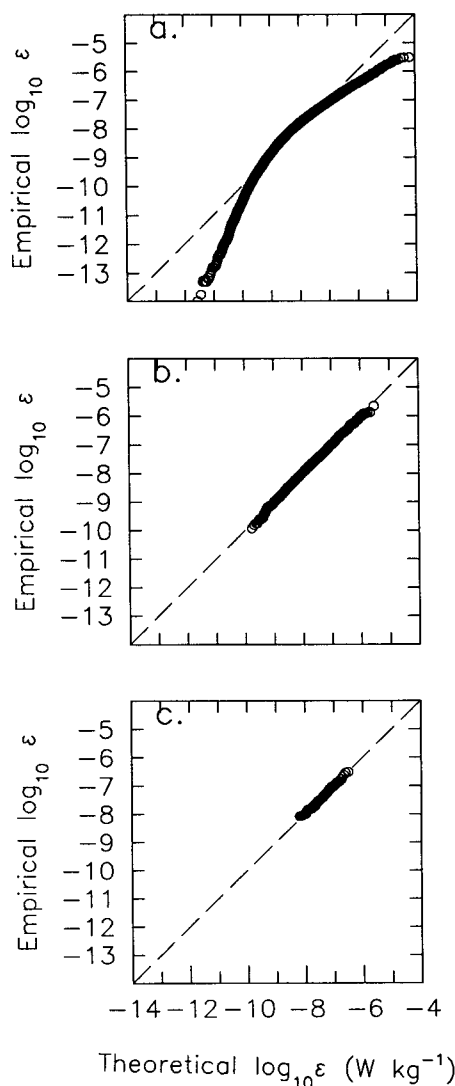


FIG. 10. The qq-plot of the instantaneous dissipation rate  $7.5\nu(\partial v/\partial z)^2$ ; (a) no averaging, (b) 4-point ( $r = 2.9\eta$ ) averaging, and (c) 64-point ( $r = 56\eta$ ) averaging.

vectively driven surface layer off the Bahamas and near the center of a warm-core ring. The data from the Bahamas passed a statistical test at a 5% level of significance, while the data from the ring failed only in a narrow region near the peak of the pdf. From a reexamination of the data, Gregg (1989, personal communication) found that the ring data were less homogeneous than the data from the Bahamas. The standard deviation of friction velocities in a benthic boundary layer (Crawford and Dewey 1990) was so small that the data passed statistical tests for *normality*.

An alternative method, which has the flexibility to be compatible with the restrictions outlined by GY, does produce dissipation estimates that distribute lognormally when the data are drawn from a single turbulent layer. Successful results were obtained with both vertical and horizontal profiles. The alternative method was not developed to be a candidate to replace the conventional method of estimating dissipation rates, rather, we developed it to show that  $\epsilon$  in the thermocline does indeed have a lognormal pdf within the scope considered by GY. The conventional and the alternative method are analogous techniques. Both produce estimates of the shear variance. The conventional method computes the variance over an explicitly controlled range of wavenumbers (or frequencies) with little control over the spatial (temporal) averaging scale. The alternative method does the same over an explicitly controlled length in space (time) with little control over the bandwidth. The alternative method may prove useful for data collected exclusively in mixing regions, where signal levels are large and the lack of bandwidth control is not serious, and it may be valuable for studies of benthic boundary layers where estimates must be made very close to the bottom (Dewey et al. 1988).

This study has shown that the lognormal pdf describes dissipation rates within a single patch of turbulence. However, the more general and important question of what is the pdf of  $\epsilon$  in the thermocline on very large scales (scales much larger than the size of an individual patch) is a more difficult one. The theory of GY provides no guidance on this general question because their concerns focussed on the inertial subrange and they did not consider the patch distribution of turbulence that has subsequently been discovered in the oceanic thermocline. A description of dissipation rates on large scales requires insight into patch statistics. In particular, we need to understand the life cycle of individual mixing events, the statistical distribution of  $\epsilon$  among an ensemble of events for all stages of their life cycle, and the distribution of the spatial scale (relative volume) of mixing events. Although this task may appear daunting, some progress has been achieved. The data reported here are a subset of a large number of profiles. A distribution formed from the mixture of two lognormal distributions passes statistical tests (Yamazaki et al. 1990) and such an heuristic approach

hints at the underlying sources of thermocline turbulence; active mixing events and decaying turbulence with unique means and standard deviations. Recently, Gregg et al. (1990) used the distribution of the fourth moment of the internal-wave shear to infer the distribution of  $\epsilon$ , having found a strong statistical correlation between these two parameters. However, turbulence is a nonlinear process; for example, it has a critical Richardson number, and there is currently no way to predict the pdf of the output of a nonlinear process from the pdf of the input. The statistical distribution of the length scale of patches has also received some attention (Gregg et al. 1986; Rosenblum and Marmorino 1990) and appears to be nearly exponential (Yamazaki and Lueck 1987).

## 5. Conclusions

The theory for the lognormal pdf of volume-averaged dissipation rates developed by Gurvich and Yaglom (1967) is valid for estimates from the oceanic thermocline when these estimates meet the restrictions set forth by Gurvich and Yaglom. These restrictions are:

- (i) the set of dissipation rates,  $\epsilon_r$ , averaged over a length scale  $r$  and drawn from a domain of spatial scale  $L$  must be statistically homogeneous,
- (ii) the averaging scale must be small compared to the domain scale,  $r \ll L$ , and
- (iii) the averaging scale must be large compared to the Kolmogorov length scale,  $r \gg \eta$ .

Dissipation rates reported previously are seldom lognormal because the conventional method of estimating  $\epsilon_r$  is usually inconsistent with these rather severe restrictions, particularly in the thermocline. The estimates are seldom homogeneous due to the patchy nature of turbulence. An alternative method that is consistent with the restrictions set forth by Gurvich and Yaglom produces estimates that have a lognormal pdf. The shortest averaging length scale that produces a lognormal pdf (condition iii) is  $3\eta$  for both a horizontal and a vertical profile taken in the thermocline.

*Acknowledgments.* We acknowledge T. R. Osborn for his encouragement and access to his data collected while he served a sentence of confinement aboard the USS *Dolphin*. We also thank the officers and crew of the USS *Dolphin* and R/V *Acania* whose skillful seamanship and dedication made this project possible. M. Gregg provided valuable comments and the annoyance expressed by one of the anonymous reviewers motivated us to clarify the original manuscript. This work was supported by the Office of Naval Research under Contracts NO.00014-87-K-0087 and NO.00014-87-K-0083.

## APPENDIX

Another Example of Instantaneous  
Dissipation Estimates

In order to demonstrate that our instantaneous dissipation method is applicable to other datasets we have examined one profile obtained with the Expendable Dissipation Profiler (XDP) during the Mediterranean Out-Flow Experiment (Lynch and Lueck 1989). The XDP (Lueck and Osborn 1985) measures one component of vertical shear,  $\partial u/\partial z$ , over wavenumber 2 to 120 cpm, and measures temperature with a spatial resolution of about 1 m. The XDP descends approximately  $2.8 \text{ m s}^{-1}$ . The data sampling for shear is made at a rate of 1024 per second, thus the maximum spatial resolution is 0.0027 m.

Because the XDP is expendable it is well suited to measurement in a benthic boundary layer. During the experiment over one hundred meters of a benthic mixing layer was observed (Fig. A1). This mixing layer was composed of two sections: an entrainment section between 340 and 410 m, and a well-mixed section between 420 m and the sea floor. These two sections are separated by a quiescent layer at 420 m. Similar features are shown in Lueck and Osborn (their Fig. 4, 1985). We use a section of shear data between 423 and 461

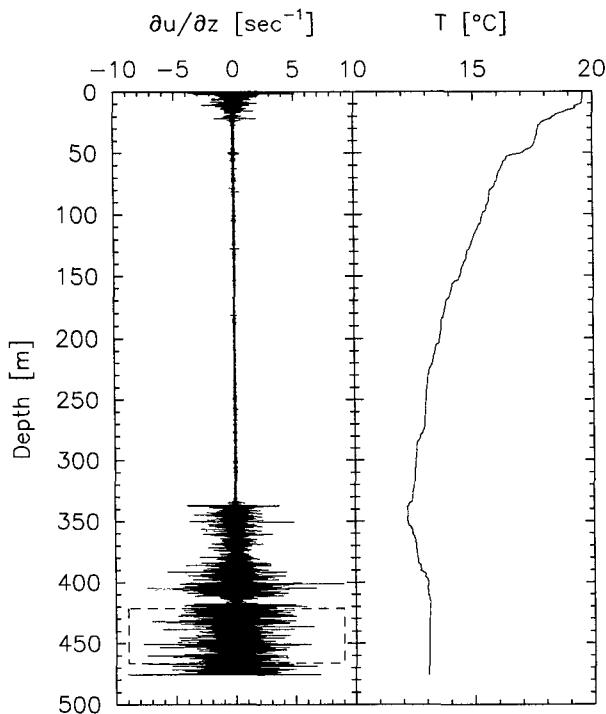


FIG. A1. Vertical shear and temperature profile measured with the XDP. The data were collected in the Gulf of Cadiz at  $35^{\circ}45'N$ ,  $6^{\circ}29'W$ . The instrument profiles right into the bottom (474 m). The benthic boundary layer is thicker than 100 m. Dashed box shows the range of data used for the instantaneous dissipation estimate.

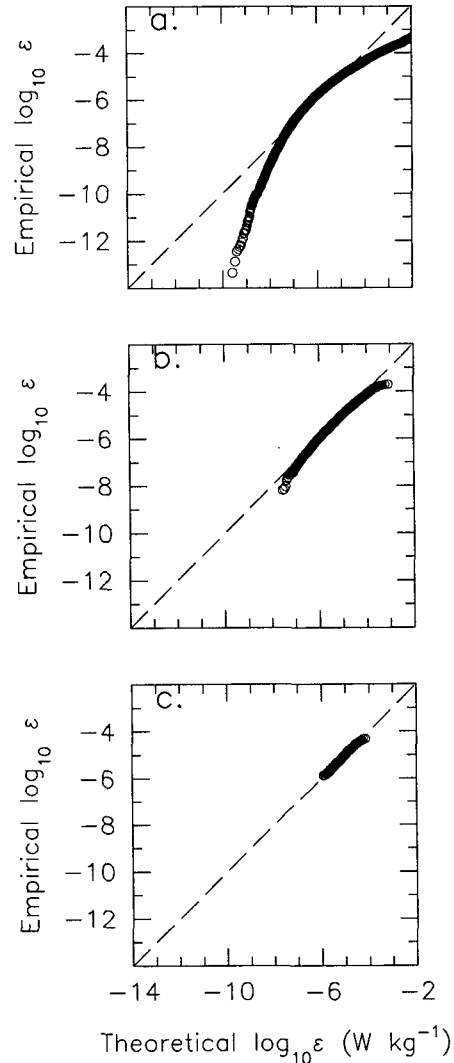


FIG. A2. The qq-plot of the instantaneous dissipation rate for the XDP: (a) no averaging, (b) 4-point averaging, and (c) 64-point averaging. Note that the range of dissipation estimates is much larger than Figs. 7 and 10.

m, which corresponds to 16 second data. The conventional spectral method using one second data gives 16 estimates of dissipation rate. The average dissipation rate from these estimates is  $1.1 \times 10^{-5} \text{ W kg}^{-1}$ , and the Kolmogorov scale,  $\eta$ , is 0.0007 m. Since the dissipation rate is extremely high, the shear spectrum is not resolved completely. As we discussed in section 3, the conventional method provides an opportunity to correct the missing part of the spectrum. The corrected dissipation average is  $2.1 \times 10^{-5} \text{ W kg}^{-1}$ , and  $\eta$  is 0.0006 m.

The raw shear data require filtering before we calculate instantaneous dissipation rates. We high-pass filtered the data at 3.6 cpm and low-pass filtered the data at 107 cpm. Unfortunately this low-pass cut off

is much lower than the Kolmogorov wavenumber, 265 cpm. Thus, we can not rigorously examine the minimum averaging scale for lognormality as done in section 3. Although we are missing the shear variance at high wavenumbers, appropriately averaged dissipation rates should follow the theory of lognormal distribution. Again, without local averaging the instantaneous dissipation estimates are not lognormal (Fig. A2a), but 4-point averaging produces lognormal samples (Fig. A2b). The 64-points averaging is also lognormal (Fig. A2c) and the averaging scale is 0.17 m, which is much shorter than the scale of the conventional method. Therefore, the instantaneous dissipation estimates can offer very detailed statistical properties of the benthic mixing layer.

## REFERENCES

- Antoniou, A., 1979: *Digital Filters: Analysis and Design*. McGraw-Hill, 524 pp.
- van Atta, C. W., and T. T. Yeh, 1975: Evidence for scale similarity of internal intermittency in turbulent flows at large Reynolds numbers. *J. Fluid Mech.*, **71**, 417–440.
- Baker, M. A., and C. H. Gibson, 1987: Sampling turbulence in the stratified ocean: statistical consequences of strong intermittency. *J. Phys. Oceanogr.*, **17**, 1817–1836.
- Chambers, J. M., W. S. Cleveland, B. Kleiner and P. A. Tukey, 1983: *Graphical Methods for Data Analysis*. Wadsworth Statistics/Probability Series, Duxbury Press, 395 pp.
- Crawford, W. R., 1982: Pacific equatorial turbulence. *J. Phys. Oceanogr.*, **12**, 1137–1149.
- , and R. K. Dewey, 1990: Confidence limits for friction velocities determined from turbulence profiles in coastal waters. *J. Atmos. Oceanic Technol.*, **7**, 50–57.
- Crow, E. L., and K. Shimizu, 1988: *Lognormal Distributions Theory and Applications*. Dekker, 387 pp.
- Dewey, R. K., P. H. LeBlond and W. R. Crawford, 1988: The turbulent bottom boundary layer and its influence on local dynamics over the continental shelf. *Dyn. Atmos. Oceans*, **12**, 143–172.
- Feller, W., 1968: *An Introduction to Probability Theory and Its Applications*, Vol. 2. John Wiley and Sons, 669 pp.
- Gargett, A. E., T. R. Osborn and P. W. Nasmyth, 1984: Local isotropy and the decay of turbulence in a stratified fluid. *J. Fluid Mech.*, **144**, 231–280.
- Grant, H. L., R. W. Stewart and A. Moilliet, 1962: Turbulence spectra from a tidal channel. *J. Fluid Mech.*, **12**, 241–268.
- Gregg, M. C., H. Seim and D. Percival, 1990: Statistics of shear and turbulence dissipation in vertical profiles. Unpublished manuscript.
- , E. A. D'Asaro, T. J. Shay and N. Larson, 1986: Observations of persistent mixing and near-inertial internal waves. *J. Phys. Oceanogr.*, **16**, 856–885.
- Gurvich, A. S., and A. M. Yaglom, 1967: Breakdown of eddies and probability distributions for small scale turbulence. *Phys. Fluids*, **10**, 59–65.
- Itsweire, E. C., and T. R. Osborn, 1988: Microstructure and vertical shear distribution in Monterey Bay. *Small-Scale Turbulence and Mixing in the Ocean*, J. C. J. Nihoul and B. M. Jamart, Eds., Elsevier Oceanogr. Ser., **46**, 213–228.
- Kolmogorov, A. N., 1941a: On the logarithmical normal particle size distribution caused by particle crushing. *Dokl. Akad. Nauk. SSSR*, **31**, 99–102.
- , 1941b: Local turbulent structure in incompressible fluids at very high Reynolds number. *Dokl. Akad. Nauk. SSSR*, **30**, 299–303.
- , 1962: A refinement of previous hypotheses concerning the local structure of turbulence in a viscous incompressible fluid at high Reynolds number. *J. Fluid Mech.*, **13**, 82–85.
- Lueck, R. G., 1988: Turbulent mixing at the Pacific subtropical front. *J. Phys. Oceanogr.*, **18**, 1761–1774.
- , and T. R. Osborn, 1985: Turbulence measurements in a submarine canyon. *Contin. Shelf Res.*, **4**, 681–698.
- Lynch, J., and R. G. Lueck, 1989: Expendable dissipation profiler (XDP) data from the Mediterranean Out-Flow Experiment: R/V *Oceanus* Cruise 202 Leg V, Tech. Rep. 92, Chesapeake Bay Institute, The Johns Hopkins University, Baltimore, Maryland, 244 pp.
- Lyubimtsev, M. M., 1976: Structure of the kinetic energy dissipation field in the ocean. *Atmos. Ocean. Phys.*, **12**, 763–764.
- Moum, J. N., and R. G. Lueck, 1985: Causes and implications of noise in oceanic dissipation measurements. *Deep-Sea Res.*, **32**, 379–390.
- , D. R. Caldwell and C. A. Paulson, 1989: Mixing in the equatorial surface layer. *J. Geophys. Res.*, **94**, 2005–2021.
- Ninnis, R., 1984: The effects of spacial averaging on airfoil probe measurements of oceanic velocity microstructure. Ph.D. thesis, University of British Columbia, Vancouver, 109 pp.
- Oakey, N. S., 1982: Determination of the rate of dissipation of turbulent energy from simultaneous temperature and velocity shear microstructure measurements. *J. Phys. Oceanogr.*, **12**, 256–271.
- Osborn, T. R., 1978: Measurements of energy dissipation adjacent to an island. *J. Geophys. Res.*, **83**, 2939–2957.
- , 1980: Estimates of the local rate of vertical diffusion from dissipation measurements. *J. Phys. Oceanogr.*, **10**, 83–89.
- , and R. G. Lueck, 1985a: Turbulence measurements from a towed body. *J. Atmos. Oceanic Technol.*, **2**, 517–527.
- , and —, 1985b: Turbulence measurement with a submarine. *J. Phys. Oceanogr.*, **15**, 1502–1520.
- Peters, H., and M. C. Gregg, 1988: Some dynamical and statistical properties of equatorial turbulence. *Small-Scale Turbulence and Mixing in the Ocean*, J. C. J. Nihoul and B. M. Jamart, Eds., Elsevier, 185–200.
- Rosenblum, L. J., and G. O. Marmorino, 1990: Statistics of mixing patches observed in the Sargasso Sea. *J. Geophys. Res.*, **95**, 5349–5357.
- Shay, T. J., and M. C. Gregg, 1986: Convectively driven turbulent mixing in the upper ocean. *J. Phys. Oceanogr.*, **16**, 1777–1798.
- Yaglom, A. M., 1966: On the influence of fluctuations in energy dissipation on the turbulence characteristics in the inertial interval. *Dokl. Akad. Nauk. SSSR*, **166**, 49–52.
- Yamazaki, H., 1990a: Breakage models: lognormality and intermittency. *J. Fluid Mech.*, **219**, 181–193.
- , 1990b: Stratified turbulence near a critical dissipation rate. *J. Phys. Oceanogr.*, **20**, 1583–1593.
- , and R. G. Lueck, 1987: Turbulence in the California undercurrent. *J. Phys. Oceanogr.*, **17**, 1378–1396.
- , —, and T. R. Osborn, 1990: A comparison of turbulence data from a submarine and a vertical profiler. *J. Phys. Oceanogr.*, **20**, 1778–1786.